in Table I, it can be concluded by simulation that the gain of a QCBP array with mixed feeding network and a conventional element array with a microstrip line feeding network is about 26.5 and 20.4 dBi, respectively. Even for the experimental array, in which LWG is used only for the first branch of the feeding network and the quasi-cavity-backed elements are used, about a 24.2 dBi gain can be achieved.

Fig. 4 shows the measured E-plane radiation pattern of both fabricated array prototypes at 29 GHz. It is observed that the improvement of the measured gain with the quasi-cavity-backed elements over the one without cavity-backed elements is about 0.62 dB, which is slightly less than the theoretical gain difference of 0.84 dB as indicated in Table I. The measured gain for the experimental QCBP array and ordinary patch array is 23.5 and 22.9 dBi, respectively. The difference of about 0.7 dB compared with the simulated result is possibly due to the mismatch of the junctions in the feeding network, which is not included in the loss analysis.

V. Conclusion

A novel configuration of integrated LTCC array antenna working in the millimeter-wave frequency band has been proposed by exploiting the flexibility of LTCC technology for 3-D integration. The antenna array uses QCBP as radiating elements. This configuration could be used in various integrated millimeter-wave antenna modules. To reduce the loss from the feeding network, a mixed feeding network configuration is proposed and verified by experiment. This communication concludes that with the LTCC multilayer technology a large scale and high gain array antenna can be built and integrated with other millimeter-wave functional components in the same ceramic tile.

Acknowledgment

The authors would like to thank the reviewers for their constructive comments and suggestions. Special thanks go to the Editors for their iterative efforts in polishing the manuscript.

References

[1] D. R. Jackson, J. T. Williams, A. K. Bhattacharyya, R. L. Smith, S. J. Buchheit, and S. A. Long, "Microstrip patch designs that do not excite surface waves," *IEEE Trans. Antennas Propag.*, vol. 41, no. 8, pp. 1026–1037, Aug. 1993.

[2] H. Uchimura, T. Takenoshita, and M. Fujii, "Development of a laminated waveguide," *IEEE Trans. Microw. Theory Tech.*, vol. 46, no. 12, pp. 2438–2443, Dec. 1998.

[3] Y. Huang, K.-L. Wu, and M. Ehlert, "An integrated LTCC laminated waveguide-to-microstrip line T-junction," *IEEE Microw. Wireless Comp. Lett.*, vol. 13, Aug. 2003.

[4] Y. Huang and K.-L. Wu, "A broadband LTCC integrated transition of laminated waveguide to air-filled waveguide for millimeter wave applications," *IEEE Trans. Microw. Theory Tech.*, vol. 51, no. 5, pp. 1613–1617, May 2003.

Parameterization of the Tapered Incident Wave for Numerical Simulation of Electromagnetic Scattering From Rough Surface

Hongxia Ye and Ya-Qiu Jin

***Abstract*—The tapered wave with the tapering parameter g has been applied to numerical simulation of electromagnetic scattering from randomly rough surface with illuminated finite surface length L. This communication presents how to select the parameters g and L, and shows quantitative relationship with the incident angle. The parameter g, as a function of incident angle, should be large enough to make the wave equation in the range of allowable error. The surface length L, larger than several correlation lengths, should be large enough to suppress the punctuated power at the surface edges and be limited to make efficient computation. Combining these criterions, a graphical format to locate g and L for different incident angle θ_i is illustrated. An empirical formula for selecting g and L as a function of θ_i is proposed.**

***Index Terms*—Forward-backward method, numerical simulation, parameterization, rough surface scattering, tapered wave.**

I. Introductions

Numerical simulation of electromagnetic scattering from randomly rough surface has been a topic of successive study for many years because of its broad applications such as terrain remote sensing, radar surveillance over oceanic surface and so on [1], [2]. The Thorsos tapered wave [3] has been extensively applied in order to circumvent artificial reflections from the edges of illuminated finite surface length. Good references can be found in Thorsos [3], Tsang [4], Kapp [5], Toporkov [6], and some others. However, how to determine the parameters of tapered incident wave in numerical computations, such as the tapering waist g, the finite surface length L and their relationship with incident angle, have been remained for further study.

This communication presents a discussion about the selection of the tapering parameters g and L with dependence upon incident angle. The tapering waist g should be large to satisfy the wave equation. The surface length L should be larger than several correlation lengths of the rough surface, minimize the edge effects, and also be limited to make computation efficiency. These requirements locate possible choices of both the parameters g and L with dependence on the incident angle, and an empirical formula for parameters criterions is summarized.

II. How to Select g and L for Tapered Incident Wave

A two-dimensional (2-D) perfectly electromagnetic conducting (PEC) randomly rough surface is shown in Fig. 1. Random surface height is given by a function $z = \xi(x)$ and its mean height $\langle \xi(x) \rangle = 0$. The matrix equation derived from the discretized MFIE with the MoM process is written as follows [7]

$$\overline{J} = \overline{J}^{i} + \overline{\overline{P}} \cdot \overline{J} \tag{1}$$

Manuscript received November 28, 2003; revised February 26, 2004. This work was supported in part by the China State Key Basis Research Project 2001CB309401-5 and in part by the China Natural Science Foundation 60171009.

The authors are with the Key Laboratory of Wave Scattering and Remote Sensing Information (LWASRSI, Ministry of Education), Fudan University, Shanghai 200433, China (e-mail: yqjin@fudan.ac.cn).

Digital Object Identifier 10.1109/TAP.2004.842586

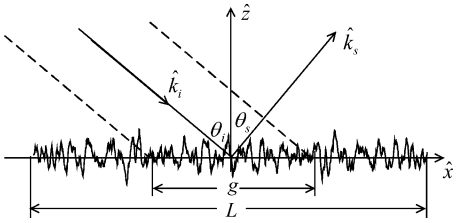

Fig. 1. Geometry of the problem.

where $\overline{J}$ is the surface current vector to be determined, $\overline{\overline{P}}$ is the kernel or propagator matrix, and $\overline{J}^i$ is the forcing term due to the incident field.

In numerical simulation of electromagnetic scattering from rough surface, the tapered wave described by the tapering parameter g has been employed to guard against the "edge effects" associated with the illuminated finite surface L. However, it seems that no certain criterion about how to select the parameters g and L has been fully presented.

Randomly oceanic rough surface is usually generated by the Pierson-Moskowitz (P-M) spectrum as follows [8]

$$W(K) = \frac{\alpha}{4|K|^3} \exp\left(-\frac{\beta g_0^2}{K^2 U^4}\right) \tag{2}$$

where K is the spatial wavenumber, $U(\mathrm{m/s})$ is the windspeed at a height of 19.5 m above the mean surface $z = 0$, $g_0 = 9.81\ \mathrm{m/s^2}$ is the gravity acceleration, and other constants $\alpha = 8.1 \times 10^{-3}$ and $\beta = 0.74$.

First, it has been known [6] that the surface length L of illuminated surface should be much larger than several correlation lengths ℓ_c, which are related to $W(K)$ with the windspeed U. Calculation finally yields

$$L > 15\ell_c = 15\frac{5}{4g_0}\sqrt{\frac{3}{\beta}}U^2 \approx 3.8U^2 \qquad (\mathrm{m}). \tag{3}$$

The Thorsos taper has been well applied because of its less computational expense. It can be written as [4]

$$\begin{aligned}\psi_i(x,z) &= T(x,z)\exp(-j\overline{k}_i\cdot\overline{r}) \\ &\equiv T(x,z)\exp\left[-jk(x\sin\theta_i - z\cos\theta_i)\right]\end{aligned} \tag{4}$$

with the taper function (see (5) at the bottom of the page) where g is the tapering parameter which directly affects the precision and validity of the scattering calculation. Thorsos [3] presented g as

$$g \gg \frac{1}{k\cos\theta_i}. \tag{6}$$

It leads to not much meaningful $g \gg 0.16\lambda$ at $\theta_i = 0^\circ$ and $g \gg 0.92\lambda$ at $\theta_i = 80^\circ$. Tsang *et al.* [4] proposed a flexible choice $g \in (L/10, L/4)$ depending on incident angle θ_i, but it can not be used for low grazing incident angle as $\theta_i \to 90^\circ$. Kapp [5] further modified (6) especially for low grazing angle as follows:

$$g > \frac{A}{k\,(\pi/2 - \theta_i)\cos\theta_i} \tag{7}$$

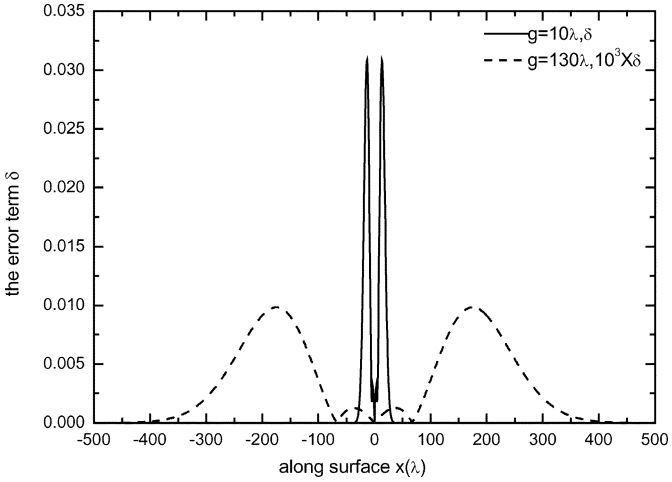

Fig. 2. Error term δ along x direction ($\theta_i = 80^\circ$).

where A is a constant, e.g., $A = 9.4$ as Toporkov suggested [6]. But it seems susceptible to have so small $g > 0.95\lambda$ at $\theta_i = 0^\circ$.

Substituting the incident tapered wave (4) into the wave equation, it yields [4]

$$\frac{\partial^2\psi_i}{\partial x^2} + \frac{\partial^2\psi_i}{\partial z^2} + k^2\psi_i = k^2\delta \tag{8}$$

where the error term

$$\begin{aligned}\delta \equiv \psi_i \Bigg\{ &-w^2 - 16\frac{(x\sin\theta_i - z\cos\theta_i)^2(x + z\tan\theta_i)^2}{k^4 g^8 \cos^6\theta_i} \\ &+ \frac{4ik(x\sin\theta_i - z\cos\theta_i)}{k^4 g^4\cos^4\theta_i}\left[1 - \frac{4(x + z\tan\theta_i)^2}{g^2}\right]\Bigg\}\end{aligned} \tag{9}$$

$$w = \frac{2\frac{(x+z\tan\theta_i)^2}{g^2} - 1}{(kg\cos\theta_i)^2}. \tag{10}$$

From (9), it can be seen that as the incident angle θ_i approaches grazing, the error term δ becomes much larger and the wave equation can not be well satisfied.

Fig. 2 shows the δ variation at $z = 0$ along $\hat{x}$ direction when $g = 10\lambda$ and $g = 130\lambda$, respectively, for $\theta_i = 80^\circ$. The peaks are correspondingly about 0.03 and 1.0×10^{-5}. Note that the dotted line for $g = 130\lambda$ is enlarged $10^3 \times \delta$ for comparison of two cases on a single figure. Large g significantly reduces the error δ.

If the incident angle θ_i is small, or the tapering parameter g takes large value, the error term δ can be significantly reduced. For example, the peak value for $\theta_i = 30^\circ$ can be reduced to 2.0×10^{-5} for $g = 10\lambda$ and 2.0×10^{-8} for $g = 100\lambda$. Supposing the permissible maximum deviation as $\delta = 10^{-4}$, the variation of g for different θ_i is numerically shown in Fig. 3. It means that g should be large and located in the shadowing region above the line to make $\delta < 10^{-4}$. Thus, a simple empirical formula is proposed to match this criterion as a function of θ_i of

$$g_{\min} = \frac{6}{(\cos\theta_i)^{1.5}}. \tag{11}$$

It is indicated by the dashed curve in Fig. 3.

$$T_T(x,z) = \exp\left\{-\frac{(x + z\tan\theta_i)^2}{g^2} - j\frac{k(x\sin\theta_i - z\cos\theta_i)}{(kg\cos\theta_i)^2}\left(\frac{2(x + z\tan\theta_i)^2}{g^2} - 1\right)\right\} \tag{5}$$

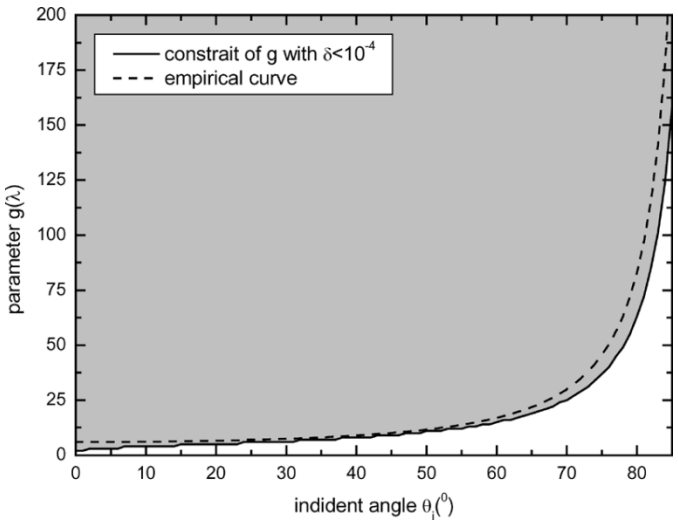

Fig. 3. Variation of g versus θ_i for $\delta = 10^{-4}$.

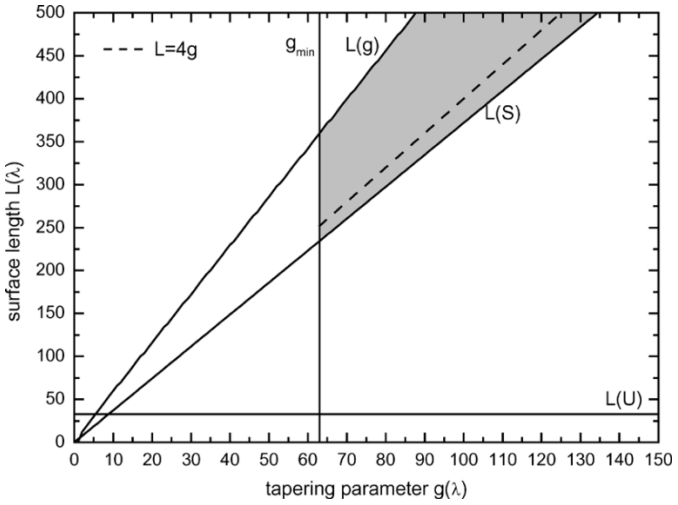

Fig. 4. To choose g and L in the shadowing area for $\theta_i = 80^\circ$.

Next issue is that at the surface edges $x = \pm L/2$, the incident power should be small enough because the energy outside the scale is neglected. It is written as [6]

$$S = 10\log_{10}\left(\frac{\left|\psi^i(L/2,0)\right|^2}{\left|\psi^i(0,0)\right|^2}\right) = -2.17\left(\frac{L}{g}\right)^2(\mathrm{dB}). \qquad (12)$$

$S \leq -30$ dB has been suggested for $\theta_i < 80^\circ$. It yields a low boundary $L(S)$ that L should be above $L(S)$.

On the other hand, to reduce computational and storage requirements, L should be limited as it can. From Fig. 2 it can be seen that the error term δ decreases quickly apart from the peak. We suggested that the surface can be truncated at such length L that the error term δ at these edges $x = \pm L/2$ arrives at 10^{-2} times of the peak value, and becomes very trivial beyond this region. It yields an upper boundary $L(g)$ that $L(S) < L < L(g)$ makes the selection of L.

Fig. 4 shows an example how to select g and L for the case of $\theta_i = 80^\circ$. Selection of g due to (11) is $g > g_{\min}$, and selection of L should be located in the shadowing region delimited by $L(g)$, $L(S)$ and $L(U)$. It is found that the dashed line defined by

$$L \geq 4g \qquad (13)$$

well satisfies these criterions.

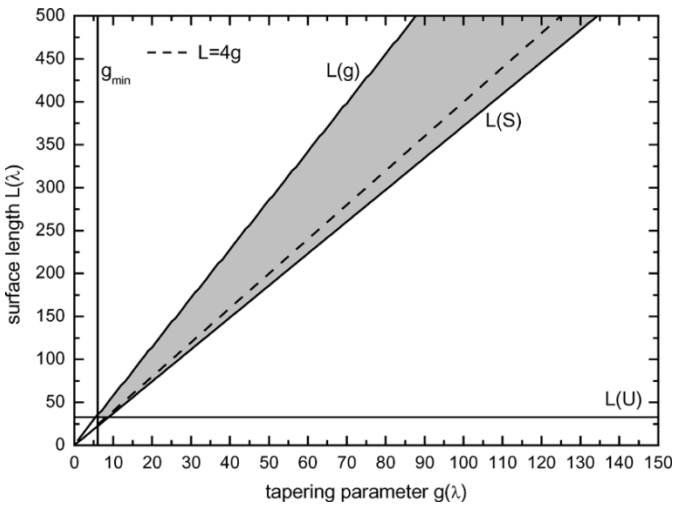

Fig. 5. To choose g and L in the shadowing area for $\theta_i = 30^\circ$.

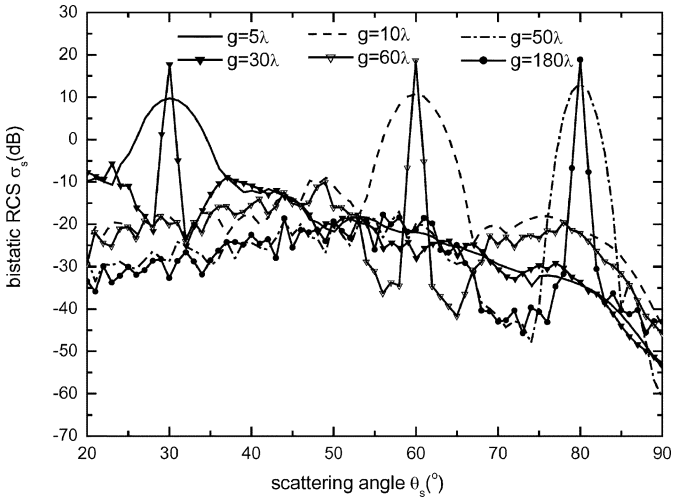

Fig. 6. Bistatic normalized RCS. ($\theta_i = 30^\circ$, $L = 120\lambda$; $\theta_i = 60^\circ$, $L = 240\lambda$; $\theta_i = 80^\circ$, $L = 700\lambda$).

Comparing with Thorsos's $g \gg 0.92\lambda$ and Kapp's $g > 50\lambda$, our criterion of (3), (11), (13), and the graphs Fig. 4 well indicate the selection of g and L.

Fig. 5 gives another example for $\theta_i = 30^\circ$. It can be seen that the parameters g and L for small θ_i can be much reduced.

III. Numerical Example of Bistatic Scattering

Fig. 6 presents the bistatic scattering from the P-M oceanic rough surface ($U = 3$ m/s) for two selected g, one is correct due to (11) and another one is too small, at respective incident angles $\theta_i = 30^\circ, 60^\circ, 80^\circ$. The value L is fixed following the correct g in each incidence case. It can be seen that the scattering peaks appear at the specular direction due to rather smooth surface ($U = 3$ m/s), especially for correct g. But, those too small g, i.e., $g = 5\lambda, 10\lambda, 50\lambda$ not following the criterion in each case, significantly damage the specular reflection pattern, because the tapered wave with too small g is not an effective approximation of the plane wave of wave equation. Specular reflection cannot appear from less coherent scattering under tapered wave incidence with too small g.

Meanwhile, our numerical results also show that as the parameters g and $L \geq 4g$ are correctly selected, further increasing $L \gg g$ does not significantly improve scattering computation. In other words, too large

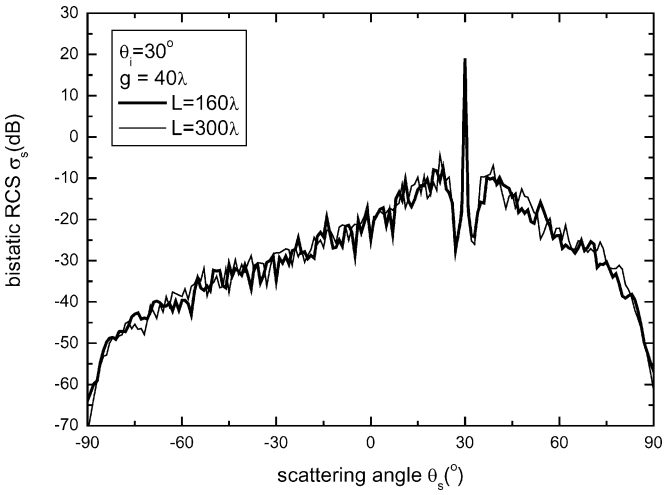

Fig. 7. Bistatic normalized RCS from different surface length L.

L seems not necessary. Fig. 7 shows an example of bistatic scattering for two $L = 160\lambda$ and $L = 160\lambda$ at $g = 40\lambda$. It can be seen that two cases are almost totally matched.

IV. Conclusion

This communication addresses the issue how to select the tapering parameter g and illuminated surface length L as a function of incident angle for numerical simulation of scattering from rough surface under tapered wave incidence. The parameter g, as a function of incident angle, should be large enough to make the wave equation in the range of allowable error. The surface length L should be larger than several correlation lengths and large enough to suppress the punctuated power at the surface edges. Also the L can be limited to make efficient computation. The criterions are simply summarized by (3), (11), (13), and are shown in the graphs for different incident angle θ_i. Numerical simulations of bistatic scattering from rough surface for correctly and not correctly selected g demonstrate the difference of angular scattering patterns.

References

[1] Y. Q. Jin and Z. Li, "Simulation of scattering from complex rough surface at low grazing angle using the GFBM/SAA method," *IEEJ Trans. Fundament. Mater. Soc. (A)*, vol. 121, no. 10, pp. 917–921, 2001.

[2] ——, "Numerical simulation of radar surveillance for the ship target and oceanic clutters in two-dimensional model," *Radio Sci.*, vol. 38, no. 3, pp. 1045–1050, 2003.

[3] E. Thorsos, "The validity of the Kirchhoff approximation for rough surface scattering using a Gaussian roughness spectrum," *J. Acoust. Soc. Amer.*, vol. 83, no. 1, pp. 78–92, 1988.

[4] L. Tsang and J. A. Kong, *Scattering of Electromagnetic Waves*. New York: Wiley, 2001, vol. 2, Numerical Simulations, pp. 118–124.

[5] D. A. Kapp, "A new numerical method for rough surface scattering calculation," Ph.D. dissertation, Virginia Polytechnic Inst. State Univ., Blacksburg, VA, 1995.

[6] J. V. Toporkov, "Study of electromagnetic scattering from randomly rough ocean-like surface using integral –equation-based numerical technique," Ph.D. dissertation, Virginia Polytech. Inst. State Univ., Blacksburg, VA, 1998.

[7] R. F. Harrington, *Field Computation by Moment Method*. New York: IEEE, 1993.

[8] W. J. Pierson and L. Moskowitz, "A proposed spectral form for fully developed wind seas based on the similarity theory of S.A. Kitaigorodskii," *J. Geophys. Res.*, vol. 69, pp. 5181–5190, 1964.

A Hybrid Method of Moments-Marching on in Time Method for the Solution of Electromagnetic Scattering Problems

Anuraag Mohan and Daniel S. Weile

***Abstract*—The time step size required by existing time-domain integral equation solvers for the solution of electromagnetic scattering problems is inversely proportional to the highest frequency present in the incident signal. This makes existing solvers inefficient, especially when the incident wave is narrowband in nature. This work presents a new time marching approach in which the time step size is inversely proportional to the bandwidth of the incident signal. The method is based on analytic signal theory and Hilbert transforms, which are used to transform the standard integral equations of electromagnetics into equations for the complex envelope of the current. Numerical results show the method to be both stable and accurate.**

***Index Terms*—Integral equations, method of moments (MoM), temporal basis functions, transient analysis.**

I. Introduction

Despite historical difficulties with efficiency and stability, time-domain integral equation (TDIE) based methods for electromagnetic simulation have received increased attention in recent years. Several methods have been proposed for making TDIE schemes more efficient [1], [2], and new techniques have either mitigated or eliminated stability problems [3]–[5]. A particularly promising technique uses a combination of band limited interpolation based on the approximate prolate spheroidal wave function with band limited extrapolation to recover causality from noncausal temporal basis functions [6], [7]. Unfortunately, all of these approaches require the time step size to be inversely proportional to the maximum frequency content of the incident wave, whereas the relevant information is contained in the bandwidth of the signal. In the scheme of [6], [7], this difficulty is exacerbated by the extrapolation scheme, which requires temporal sampling at about ten times the Nyquist rate to ensure its accuracy. For narrowband signals, such those that arise in communications and continuous wave radar applications, the waste inherent in modeling a broad frequency band when only narrowband data is needed can be immense.

This paper proposes to alleviate this inefficiency by representing temporally bandlimited signals using analytic signal theory [8], which is an extension of the familiar frequency-domain phasor theory to the time-domain. Doing so enables an incident bandpass signal to be represented by only its envelope, so that only the true frequency support of the signal need be represented. For relatively narrowband signals, this can vastly increase the time step size. Finally, the discussion presented below will demonstrate that the new method is actually a combination of the TDIE method with the frequency domain method of moments (MoM), and that it can be reduced to either with only small changes to the formulation.

The remainder of this paper will proceed as follows: Section II will discuss the formulation and discretization of TDIEs in the phasor (that is, analytic signal) domain. Numerical results verifying the accuracy, efficiency, and stability of the method of Section II will be presented

Manuscript received July 19, 2004. This work was supported by the National Science Foundation under Grant ECS-0348109.

The authors are with the Department of Electrical and Computer Engineering, University of Delaware, Newark, DE 19716 USA (e-mail: mohan@mail.eecis.udel.edu).

Digital Object Identifier 10.1109/TAP.2004.842581